Solitary synchronization waves in distributed oscillator populations

L. A. Smirnov,[1,2] G. V. Osipov,[1] and A. Pikovsky[1,3]
[1]*Department of Control Theory, Nizhny Novgorod State University, Gagarin Ave. 23, 606950, Nizhny Novgorod, Russia*
[2]*Institute of Applied Physics, Ul'yanov Str. 46, 603950, Nizhny Novgorod, Russia*
[3]*Institute for Physics and Astronomy, University of Potsdam, Karl-Liebknecht-Str. 24/25, D-14476 Potsdam-Golm, Germany*

(Received 3 August 2018; published 27 December 2018)

We demonstrate the existence of solitary waves of synchrony in one-dimensional arrays of oscillator populations with Laplacian coupling. Characterizing each community with its complex order parameter, we obtain lattice equations similar to those of the discrete nonlinear Schrödinger system. Close to full synchrony, we find solitary waves for the order parameter perturbatively, starting from the known phase compactons and kovatons; these solutions are extended numerically to the full domain of possible synchrony levels. For nonidentical oscillators, the existence of dissipative solitons is shown.

DOI: 10.1103/PhysRevE.98.062222

I. INTRODUCTION

The dynamics of oscillator populations attracts much interest across different fields of science and engineering. The paradigmatic and universal object of study is the Winfree-Kuramoto model of globally coupled phase oscillators. It demonstrates a transition to synchrony, characterized in terms of the Kuramoto order parameter [1]. This effect is relevant to many systems (lasers, biocircuits, and electronic and electro-chemical oscillators [2]), which can be well described within the mean-field coupling models. In the case where the oscillators are organized as an ordered medium or a lattice with a distant-dependent coupling, spatiotemporal patterns can be observed. The most popular are standing chimera states, where regions of synchrony and asynchrony coexist [3], first reported for a one-dimensional (1D) medium by Kuramoto and Battogtokh (KB) [4]. The smallest system to observe chimera experimentally is that of two or three lumped subpopulations [5]. Further experiments have been performed with media of nonlocally coupled chemical oscillators [6] (up to 1600 units).

While 1D chimera patterns are typically stationary solutions, a size of which is a characteristic system size, a possibility of localized traveling waves of the complex order parameter in oscillatory media remains an open problem. In this paper we report on solitary synchronization waves in an 1D oscillatory medium with Laplacian coupling. Our first model—a lattice of subpopulations of phase oscillators—can be interpreted as a lattice generalization of systems of two and three coupled oscillator communities, extensively studied in Refs. [7,8]. The main tool of our analysis is based on the Ott-Antonsen (OA) ansatz [9], allowing one to write closed equations for the complex order parameter (see Ref. [10] for applications of this ansatz to the KB-type chimeras). The resulting model resembles the nonlinear Schrödinger (NLS) lattice [11]; thus our model provides a link between the theory of synchronization and the theory of solitons. We find solitary waves in the lattice via a perturbation method, starting with compacton solutions for the fully synchronous case, and describe the full domain of existence of localized waves for different levels of synchrony. Furthermore, we show that for 1D arrays with diversity of natural frequencies and with additional attractive coupling compensating this diversity, waves of synchrony exist as dissipative solitons. To show the generality of synchrony waves, we also demonstrate them in an off-lattice model of a continuous oscillatory medium with an interaction defined through a convolution integral. In contradistinction to the KB setup, the interaction kernel is of Laplacian type, the integral over which vanishes.

II. TRAVELING WAVES IN A LATTICE MODEL

A. Network of nearest-neighbor interacting subpopulation of globally coupled phase oscillators

As a starting point, we consider an infinite 1D lattice (index n) of nearest-neighbor interacting subensembles of M globally coupled (in general, nonidentical) elements (index m). In this case, the evolution of the phase $\varphi_{nm}(t)$ of the mth unit belonging to population n is given by

$$\frac{d\varphi_{nm}}{dt} = \omega_{nm} + \sum_{\tilde{n}=n-1}^{n+1} \frac{K_{n\tilde{n}}}{M} \sum_{\tilde{m}=1}^{M} \sin\left(\varphi_{\tilde{n}\tilde{m}} - \varphi_{nm} - \alpha_{n\tilde{n}}\right), \quad (1)$$

where ω_{nm} is the natural frequency of the mth oscillator in community n, $K_{n\tilde{n}}$ is the strength, and $\alpha_{n\tilde{n}}$ is the phase lag of coupling between the oscillators in group n and those in group $\tilde{n}$. Such a model in the case of two coupled populations is known as the Abrams *et al.* model, possessing chimera states and intensively studied recently (see Refs. [7,8] for the theoretical analysis of two and tree populations, and Ref. [5] for experimental realizations). Typically, frequencies ω_{nm} obey a known distribution $g(\omega)$. Following the works [7–9], we take $g(\omega)$ to be the Cauchy distribution $\pi g(\omega) = \gamma[(\omega-\omega_0)^2+\gamma^2]^{-1}$. Here we assume that each subpopulation is coupled only to the two nearest-neighbor communities symmetrically with $K_{n(n\pm1)} = \kappa$, $\alpha_{n(n\pm1)} = \alpha$, and to itself with $K_{nn} = -2(\kappa+\varkappa)$, $\alpha_{nn} = \alpha+\beta$. Noteworthy, we may set $\kappa = 1$ by rescaling time.

The macroscopic state of the nth population is fully characterized by the local Kuramoto order parameter $Z_n = M^{-1}\sum_{m=1}^{M} e^{i\varphi_{nm}}$. Physically, the amplitude of this complex parameter describes the level of synchrony of the units belonging to group n: $|Z_n| = 0$ if the phases are uniformly distributed (full asynchrony), and $|Z_n| = 1$ in the case of full synchrony where the phases coincide. Partial coherence of oscillators corresponds to $0 < |Z_n| < 1$. In the case of infinitely large number M of particles per each community, one can reduce the problem, using the OA ansatz [7–9], to lattice equations with nearest-neighbor Laplacian coupling for $Z_n(t)$. The main steps of the procedure for deriving these equations are as follows.

In the so-called thermodynamic limit $M \to \infty$, it is natural that the nth continuum of phase oscillators at each ω value and at the time t can be characterized by its own probability density function $f_n(\varphi, \omega, t)$, which evolves according to the continuity equation

$$\frac{\partial f_n}{\partial t} + \frac{\partial}{\partial \varphi}(u_n f_n) = 0, \tag{2}$$

where $u_n(\varphi, \omega, t)$ represents the instantaneous velocity of elements in population n and is respectively determined by the expression

$$u_n = \omega + \mathrm{Im}[H_n(t)e^{-i\varphi}], \quad H_n = \sum_{\tilde{n}=n-1}^{n+1} K_{n\tilde{n}} e^{-i\alpha_{n\tilde{n}}} Z_{\tilde{n}}. \tag{3}$$

Here we introduce an auxiliary macroscopic field $H_n(t)$, which describes the force on subgroup n.

According to the OA approach [7–9], we use a special ansatz for the expansion of $f_n(\varphi, \omega, t)$ in a Fourier series with respect to φ in the form of a Poisson kernel

$$f_n(\varphi, \omega, t) = \frac{\mathrm{g}(\omega)}{2\pi}\left\{1 + \sum_{q=1}^{\infty}\left[a_n^q(\omega, t)e^{iq\varphi} + \mathrm{c.c.}\right]\right\} \tag{4}$$

(c.c. stands for the complex conjugate). After the substitution of relations (3) and (4) into Eq. (2), we arrive at an exact solution, so long as $a_n(\omega, t)$ satisfies the equality

$$\frac{\partial a_n}{\partial t} + i\omega a_n + \frac{1}{2}\left[a_n^2 H_n(t) - H_n^*(t)\right] = 0. \tag{5}$$

Then we take into account that the local order parameter $Z_n(t)$ essentially represents the average of the complex numbers $e^{i\varphi_{nm}}$ over all phase oscillators belonging to community n, and it is therefore generalized [with the help of probability density function $f_n(\varphi, \omega, t)$] as an integral in the limit where $M \to \infty$. Hence, one can express $Z_n(t)$ in terms of the OA manifold (4). Moreover, it is possible to evaluate $Z_n(t)$ analytically by contour integration, yielding to $Z_n(t) = a_n^*(\omega_0 - i\gamma, t)$, if we use the assumption that the natural frequencies ω_{nm} are selected independently from the Cauchy distribution with the width γ and the mean ω_0 (the latter can be set to zero by virtue of a transformation to the rotating reference frame, i.e., below $\omega_0 = 0$ except in special cases).

Finally, considering the right-hand side of (5) at the poles $\omega = \omega_0 - i\gamma$, in the mesoscopic formulation we obtain the following discrete system of coupled equations for the complex order parameters $Z_n(t)$ of subpopulations:

$$\frac{dZ_n}{dt} = (i\omega_0 - \gamma)Z_n + \frac{1}{2}\left(H_n - H_n^* Z_n^2\right),$$
$$H_n = e^{-i\alpha}(Z_{n-1} + Z_{n+1} - 2Z_n) + \mu Z_n. \tag{6}$$

From (6) it is clearly seen that the phase shift α determines whether the Laplacian coupling is attractive, repulsive, or neutral. Here the complex parameter $\mu = \mu_r + i\mu_i = 2e^{-i\alpha}[1 - (1 + \varkappa)e^{-i\beta}]$ defines the level of an additional local (within the site n) interaction. Below we focus on the traveling waves, and therefore the lattice is considered as an infinite one; in numerics the system is taken much larger than the domain depicted in figures, thus the boundary effects are irrelevant.

B. Waves in a lattice with conservative coupling

1. Linear waves

We start with the conservative case: first, we set $\mu = 0$ and $\alpha = -\pi/2$, corresponding to a neutral coupling; and second, we assume all the oscillators to be identical, i.e., $\gamma = 0$. In this case, spatially uniform solutions have the form $Z_n = \varrho e^{i\psi}$ with any $0 \leqslant \varrho \leqslant 1$, i.e., any level of homogeneous synchrony is possible. Linear waves $\propto e^{iwt-ikn}$ on top of such a background have dispersion

$$w(k) = \sqrt{1 - \varrho^4}(1 - \cos k). \tag{7}$$

The phase velocity λ_{ph} and group velocity λ_{gr} of the linear waves described by this dispersion are determined by the following relations $\lambda_{\mathrm{ph}} = \sqrt{1 - \varrho^4}(1 - \cos k)/k$ and $\lambda_{gr} = \sqrt{1 - \varrho^4}\sin k$, respectively.

2. Compactons and kovatons

We now look for nonlinear solitary waves; the only parameter is the homogeneous level of synchrony ϱ. It is instructive to start with the degenerate case of full synchrony $\varrho = 1$. As it follows from relation $w(k)$, in this case there are no linear waves. In fact, because $|Z_n| = 1$, the only nontrivial variable is the phase of the complex order parameter, and the equation for this phase is the same as for a lattice of neutrally coupled phase oscillators, studied in Ref. [12]. With $Z_n = e^{i\Theta_n}$ and $V_n = \Theta_n - \Theta_{n-1}$, the dynamical equations can be reduced to a simple lattice system

$$\frac{dV_n}{dt} = \cos V_{n+1} - \cos V_{n-1}. \tag{8}$$

Solitary waves in this fully synchronous lattice, compactons and kovatons, have been thoroughly analyzed in Ref. [12]; here we briefly outline their main features. Traveling waves $V_n(t) = V(\tau)$, where $\tau = t - n/\lambda$, can be either compact one-hump pulses (compactons) with velocities $0 < \lambda < \lambda_c = 4/\pi$, or extended domains (kovatons) between two compact kinks, connecting states $V = 0$ and $V = \pi$, with velocity $\lambda = \lambda_c$. To find the form of a localized solution moving with a constant velocity λ, we posit $V_n(t) = V(\tau)$ in (8) and arrive at a delay-advanced equation. Integration of this equation yields

$$V(\tau) = \int_{\tau-b}^{\tau+b} [1 - \cos V(\tilde{\tau})]\, d\tilde{\tau}. \tag{9}$$

Here $b = 1/\lambda$, and the choice of the integration constant ensures that $v = 0$ is a solution. Then we numerically solve

Eq. (9) using the Petviashvili iteration method [12]. This allows us to determine numerically traveling waves in the whole range of velocities $0 < \lambda \leqslant \lambda_c = 4/\pi$.

3. Solitary waves close to compactons

Next, in the framework of Eqs. (6), we look for solitary waves moving with constant velocities on top of a partially synchronous homogeneous background with $\varrho < 1$. Substituting $Z_n = \rho_n e^{i\theta_n}$ in (6), we obtain a system

$$\frac{d\rho_n}{dt} = \frac{(1-\rho_n^2)}{2}(\rho_{n-1}\sin v_n - \rho_{n+1}\sin v_{n+1}), \tag{10a}$$

$$\frac{d\theta_n}{dt} = \frac{(1+\rho_n^2)}{2\rho_n}(\rho_{n-1}\cos v_n + \rho_{n+1}\cos v_{n+1} - 2\rho_n), \tag{10b}$$

where $v_n = \theta_n - \theta_{n-1}$. We employ a traveling wave ansatz $\rho_n(t) = \rho(\tau)$ and $\theta_n(t) = \theta(\tau)$ where $\tau = t - nb$, and $b = 1/\lambda$ is the inverse velocity, and we also assume that $\rho(\tau)$ and $\theta(\tau)$ satisfy conditions $\rho(-\infty) = \rho(+\infty) = \varrho$, $\theta(-\infty) = \theta^-$, $\theta(+\infty) = \theta^+$ (θ^- and θ^+ are two constants). In this case, for convenience of the further analysis, it is useful to introduce auxiliary variables $r(\tau) = \rho(\tau) - \varrho$ and $v(\tau) = \theta(\tau) - \theta(\tau + b)$, which both tend to zero at $\tau \to \pm\infty$: $r(\pm\infty) = 0$ and $v(\pm\infty) = 0$. As a result, with the traveling wave ansatz, the discrete lattice equations (10) reduce to delay-advanced differential equations for the waveform $r(\tau)$ and $v(\tau)$:

$$\frac{dr(\tau)}{d\tau} = \frac{\{1-[\varrho + r(\tau)]^2\}}{2}\{\varrho[\sin v(\tau) - \sin v(\tau - b)] + r(\tau + b)\sin v(\tau) - r(\tau - b)\sin v(\tau - b)\}, \tag{11a}$$

$$\frac{dv(\tau)}{d\tau} = \frac{\{1+[\varrho + r(\tau)]^2\}}{2\{\varrho + r(\tau)\}}\{2\varrho[\cos v(\tau) + \cos v(\tau - b) - 1] + r(\tau + b)\cos v(\tau) + r(\tau - b)\cos v(\tau - b) - 2r(\tau)\} - \frac{\{1+[\varrho + r(\tau + b)]^2\}}{2[\varrho + r(\tau + b)]}\{2\varrho[\cos v(\tau + b) + \cos v(\tau) - 1] + r(\tau + 2b)\cos v(\tau + b) + r(\tau)\cos v(\tau) - 2r(\tau + b)\}. \tag{11b}$$

We develop a perturbation approach allowing finding solutions analytically for the case close to synchrony $\varrho \lesssim 1$. Introducing a small parameter $\epsilon = (1 - \varrho) \ll 1$, we write $r(\tau) = \epsilon r_1(\tau) + o(\epsilon^2)$, $v(\tau) = V(\tau) + \epsilon v_1(\tau) + o(\epsilon^2)$. Here $V(\tau) = V_n(t)$ is a compacton solution of (8). Substituting these asymptotic expansion in ϵ into Eqs. (11a) and (11b) into the first order smallness in ϵ, we obtain the following linear inhomogeneous delay-advanced differential equations for functions $r_1(\tau)$ and $v_1(\tau)$, respectively:

$$\frac{dr_1(\tau)}{d\tau} = [1 - r_1(\tau)][\sin V(\tau) - \sin V(\tau - b)], \tag{12a}$$

$$\frac{dv_1(\tau)}{d\tau} = v_1(\tau + b)\sin V(\tau + b) - v_1(\tau - b)\sin V(\tau - b) + g(\tau), \tag{12b}$$

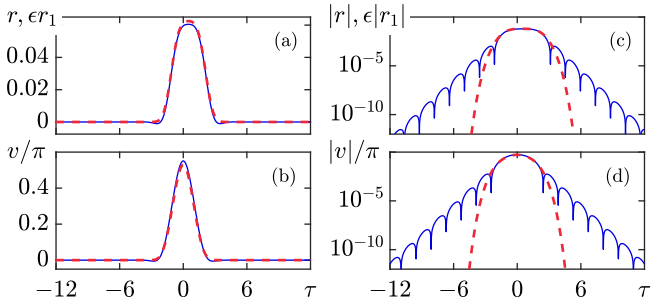

FIG. 1. Numerically obtained form $r(\tau)$ and $v(\tau)$ (solid blue line) of the soliton for $\lambda = 1.01862$ and $\varrho = 0.9$ compared with the leading approximation (13) and $V(\tau)$ (red dashed line). In the logarithmic scale (b, d) one can clearly see exponentially decaying tails with oscillations.

where $g(\tau)$ reads

$$g(\tau) = [r_1(\tau + b) - r_1(\tau)][2 + \cos V(\tau)] + [r_1(\tau - b) - 1] \times \cos V(\tau - b) + [1 - r_1(\tau + 2b)]\cos V(\tau + b).$$

Most important is the evolution of the correction $\epsilon r_1(\tau)$ to the constant value ϱ, so we consider only it below. Equation (12a) allows us to represent $r_1(\tau)$ as an integral over the compacton waveform

$$r_1(\tau) = 1 - \exp\left\{\int_{-\infty}^{\tau}[\sin V(\tilde{\tau} - b) - \sin V(\tilde{\tau})]\,d\tilde{\tau}\right\}. \tag{13}$$

In this approximation the profile $r_1(\tau)$ is as compact as the compacton of (8), i.e., it has superexponentially decreasing tails. The exact localized solution of system (10) has exponentially decaying tails like usual solitons, because for $\varrho < 1$ this system possesses also linear waves. We compare the approximate solution with the numerical solitary wave in Fig. 1.

4. General traveling localized wave

For general parameters ϱ and λ, we solve system (11) for localized solutions numerically. Starting from an approximation obtained analytically as outlined above, we apply an iterative procedure based on the Newton method to find an exact fixed point of these equations. The strategy is to start from solutions very close to synchrony (i.e., $\varrho \lesssim 1$), where the shape of the solitary wave is known from the perturbation approach and to change parameters gradually to remain in the convergence domain of the Newton method. In this way, solitons can be found in a large range of parameters, and the borders of these ranges can be identified; see Fig. 2. There we also illustrate shapes of solitary waves. Typical are one-hump $r(\tau)$ profiles for small velocities, and two-hump profiles for large λ [Figs. 2(b) and 2(c)]. Tails of the solitons become more wavy close to the lower border, which is essentially determined by the resonance with the phase velocity $\lambda_{\rm ph}$ of linear waves. Close to the top border, the solitons look like extended domains bounded by two humps [Figs. 2(d) and 2(e)]. All such solitons [which are essentially formed by two kinks of variable $v(\tau)$ that connect the states with $v = 0$ and $v = v_* \lesssim \pi$] possess nearly the same height and the same speed, but their width is not fixed. This feature is similar to

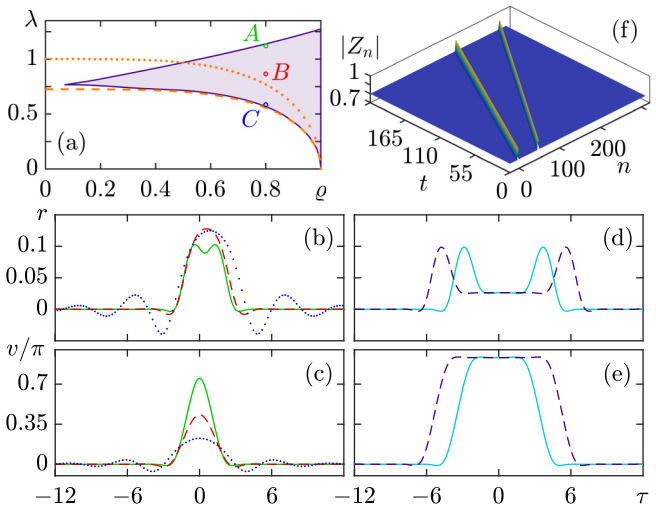

FIG. 2. (a) Existence region (shadowed) of solitons. The dashed and the dotted lines represent the maximal phase and group velocities of the linear waves, respectively. (b, c) Solitons for $\varrho = 0.8$ and three different velocities: $\lambda = 1.12096$ (green solid line, point A in panel a), $\lambda = 0.85829$ (red dashed line, point B), and $\lambda = 0.58404$ (blue dotted line, point C). (d, e) Two solitary waves having different widths, moving with practically the same constant velocity $\lambda = 1.13952$ on top of a homogeneous background with $\varrho = 0.8$. (f): Space-time dynamics of two solitons with $\lambda = 1.12096$ and $\lambda = 0.85829$.

the properties of kovatons in model (8). The maximal group velocity $\lambda_{gr}^{\max}$ of linear waves is not essential for the existence of solitons, but rather for their visibility. From a compact initial profile, solitons with velocity larger than $\lambda_{gr}^{\max}$ dominate the front edge zone; this occurs for $\varrho \gtrsim 0.5015$.

In Fig. 2(f) we show the results of direct numerical simulations within the conservative case of the lattice (6), starting from the solutions obtained by the Newton method. Solitons are stable and do indeed propagate with constant velocities and permanent shapes.

C. Destruction of waves due to dissipation and formation of dissipative solitons

Above we have considered oscillator arrays with purely conservative coupling. For $|\alpha| \lesssim \pi/2$ the linear waves decay, and one can expect that the solitons decay as well. We illustrate this in Fig. 3. Here we start with a soliton found for $\alpha = -\pi/2$; during the propagation it gets destroyed.

Generally, there is another source of synchrony "nonconservation." This is a diversity of oscillators, in particular of their natural frequencies, characterized by parameter γ. Desynchronizing effect of diversity can be compensated by a local synchronizing coupling described by parameter μ in (6). For $\gamma \neq 0$, $\mu \neq 0$, only one uniform level of synchrony is possible, given by the stationary solution of Eq. (6) with $H_n = \mu Z_n$: $\varrho_* = \sqrt{(\mu_r - 2\gamma)/\mu_r}$. In Fig. 4 we show what happens to a localized initial perturbation in such a system. Here we choose γ and μ in such a way that the homogeneous state has the same level of synchrony $\varrho_* = 0.8$ and start with the same initial condition as in Fig. 3. After an initial transient, this solution evolves into a localized wave which is not similar to

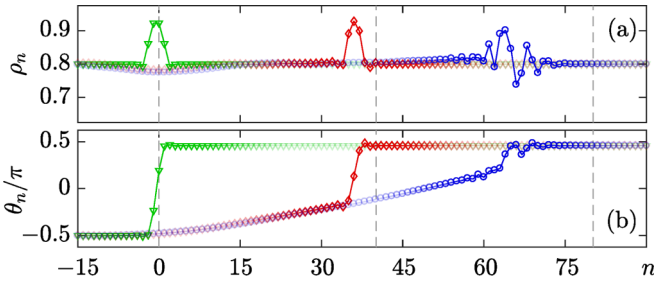

FIG. 3. Evolution of the initial soliton (green line with triangles), calculated for $\varrho = 0.8$ and $\lambda = 0.85307$ in a lattice (6) with slightly nonconservative coupling $\alpha = -0.496\pi$. Profile at $t = 47$ is in red with diamonds, profile at $t = 94$ is in blue with circles. The dashed vertical lines show the soliton positions if $\alpha = -\pi/2$, to illustrate deceleration. The amplitude of the soliton decreases, and the oscillating tails become visible.

the conservative soliton, but nevertheless appears to be stable and propagates with a constant velocity and a permanent form. This solution can be attributed as a dissipative solitary synchronization wave. In Fig. 5 we also show with direct numerical simulations how the found dissipative soliton of the complex order parameter propagates in a chain of the interacting communities (1). One can see that the solitary wave is robust despite the finite-size deviations from the OA description.

III. SOLITARY WAVES IN A CONTINUOUS OSCILLATORY MEDIUM

Above we have formulated the simplest model for Laplacian coupling as a lattice of subpopulations; however, spatially continuous systems with nonlocal coupling have similar properties (this is a well-known correspondence between lumped and continuous systems). The setup we employ is close to the KB model of a 1D oscillatory medium [4]:

$$\frac{\partial \varphi}{\partial t} = \mathrm{Im}(He^{-i\varphi}), \quad H(x,t) = e^{-i\alpha} \int G(x-\tilde{x}) e^{i\varphi(\tilde{x},t)}\, d\tilde{x}. \tag{14}$$

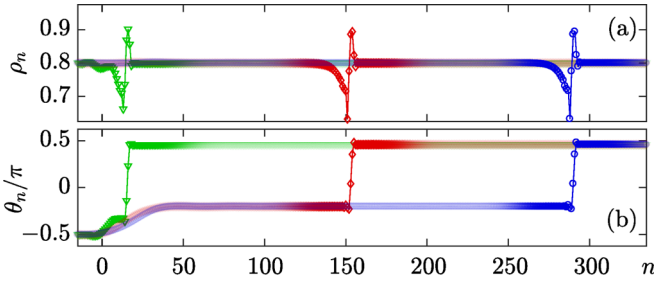

FIG. 4. Formation of a dissipative soliton, moving with a constant velocity $\lambda_{ds} \approx 0.72$. Snapshots at $t = 20$ (green line with triangles), $t = 210$ (red line with diamonds), and $t = 400$ (blue line with circles) for the numerical simulations of Eq. (6) with $\alpha = -\pi/2$, $\mu = 0.26 - 0.0595i$, $\gamma = 0.0468$, and $\omega_0 = 0.04879$. Initial conditions: a conservative soliton having velocity $\lambda = 0.85307$ and propagating on top of a homogeneous background with $\varrho = 0.8$.

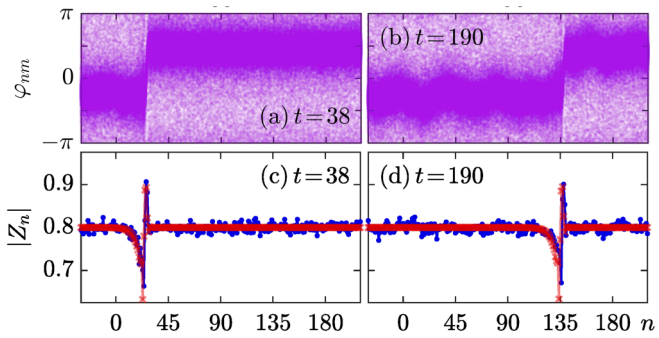

FIG. 5. Solitary wave simulated in a chain of oscillator populations (1) with $\alpha = -\pi/2$, $\beta = -0.1256$, $\varkappa = 0.037927$, $\gamma = 0.0468$, and $\omega_0 = 0.04879$, where each population consists of $M = 2000$ coupled elements. (a, b) Instantaneous phases. (c, d) Amplitude of the complex order parameter (blue line with dots) compared with solution of (6) (red line with crosses). Initial conditions: randomized phases generated according to the OA theory and yielding the same profile of Z_n as the dissipative soliton of Fig. 4 has.

Here we assume all oscillators to be identical, so that their natural frequency can be set to zero by virtue of a transformation to the rotating reference frame. Note, the integral in (14) is understood in the Lebesgue sense so that no spatial smoothness of function $e^{i\varphi(x,t)}$ is needed. In Ref. [4] as well as in many other studies of chimera patterns [3,13], the interaction was assumed to be of a mean-field type, characterized by a nonzero mean strength $\int G(x)dx \neq 0$. Here, in contradistinction, we choose a Laplacian symmetric coupling with a vanishing mean value: $\int G(x)\,dx = 0$. The prototypic example of such a kernel is the second-order derivative of the Gaussian

$$G(x) = \mathcal{A}\sigma^{-4}(x^2 - \sigma^2)e^{-x^2/2\sigma^2}, \tag{15}$$

where $\mathcal{A}$ is an amplitude (which determines the timescale and thus can be arbitrary), and σ is a characteristic width of this function (it is convenient for the further numerical analysis not to set $\sigma = 1$ but to keep it as a parameter).

The analogy to the lattice model (6) becomes evident if one introduces the coarse-grained complex order parameter $Z(x,t) = \langle e^{i\varphi(x,t)}\rangle$, where the averaging is performed over an infinitesimally small neighborhood of site x. For $Z(x,t)$ one can apply the OA reduction [3,9] to obtain

$$\frac{\partial Z}{\partial t} = \frac{1}{2}(H - H^* Z^2),$$
$$H(x,t) = e^{-i\alpha}\int G(x-\tilde{x})Z(\tilde{x},t)\,d\tilde{x}. \tag{16}$$

Noteworthy, the Lebegues integral over a nonsmooth phase profile in (14) is transformed, by virtue of coarse graining, to the Cauchy integral over the smooth order parameter in (16). The integro-differential equation (16) is a continuous counterpart of the lattice system (6) for identical elements. Actually, the discrete model (6) considered above (with $\gamma = 0$ and $\beta = 0$) captures all the essential properties of Eq. (16) and can be viewed as a simplification of the continuous model (16), where a temporary instantaneous, integral relation between $Z(x,t)$ and $H(x,t)$ is replaced by a nearest-neighbor Laplacian coupling. From this formal point of view, the spatial index n in (6) describes domains (of the characteristic size σ) that contribute to the coupling field H as "coarse-grained macroscopic lattice sites." The discrete OA equation (6) and the corresponding system (1) for a nearest-neighbor interacting network of phase oscillators, where at each site n there is a large population of M units, are most suitable for the analytical and numerical analysis of solitary synchronization waves, however, we now present numerical evidence of such traveling waves for Eq. (16) and the KB model (14) of a 1D oscillatory medium with nonlocal interaction characterized by the kernel (15).

Existence of solitary synchronization waves appears to be a general property of 1D media with Laplacian coupling, both discrete ones (6) and continuous ones (16). To find within the framework of Eq. (16) spatially inhomogeneous localized structures moving at constant velocities λ against a homogeneous partially coherent background ϱ, we again employ the traveling wave ansatz $Z(x,t) = Z(\xi)$, $H(x,t) = H(\xi)$, where $\xi = x - \lambda t$. We represent the complex order parameter $Z(\xi)$ and the coupling field $H(\xi)$ in the form $Z(\xi) = \rho(\xi)e^{i\theta(\xi)}$, $H(\xi) = h(\xi)e^{i\psi(\xi)}$, where $\rho(\xi)$, $\theta(\xi)$, $h(\xi)$ and $\psi(\xi)$ are real-valued functions of ξ. Substituting this in (16) and introducing auxiliary variables $r(\xi) = \rho(\xi) - \varrho$ and $v(\xi) = d\theta/d\xi$, that both tend to zero at $\xi \to \pm\infty$, we get a system of integro-differential equations for $r(\xi)$ and $v(\xi)$:

$$\frac{dr}{d\xi} = -\frac{h[1-(\varrho+r)^2]}{2\lambda}\cos(\psi-\theta), \tag{17a}$$
$$\frac{dv}{d\xi} = -\frac{[1+(\varrho+r)^2]}{2\lambda(\varrho+r)}\left[\frac{dh}{d\xi}\sin(\psi-\theta) + h\frac{d\psi}{d\xi}\cos(\psi-\theta)\right] - \frac{h^2[1+(\varrho+r)^4]}{4\lambda^2(\varrho+r)^2}\sin(2\psi-2\theta). \tag{17b}$$

Here $\theta(\xi)$, $h(\xi)$, and $\psi(\xi)$ can be found from the following integral relations:

$$\theta(\xi) = \int_{-\infty}^{\xi} v(\tilde{\xi})\,d\tilde{\xi}, \tag{18}$$
$$h(\xi)e^{i(\psi(\xi)+\alpha)} = \int_{-\infty}^{+\infty} G(\xi-\tilde{\xi})[\varrho + r(\tilde{\xi})]e^{i\theta(\tilde{\xi})}\,d\tilde{\xi}. \tag{19}$$

We would like to note that it is convenient to use variables $r(\xi)$ and $v(\xi)$ in numerical calculations, because we assume that $r(\pm\infty) = 0$ and $v(\pm\infty) = 0$.

From (17)–(19), one can pass, using the standard discretization procedure, to a system of nonlinear equations for fixed values of the parameters ϱ and λ. We employ the Newton iterative algorithm to numerically find a fixed point of such a large-dimension system. It allows us to approximate (with high precision) a localized solution of Eqs. (17) with additional conditions (18) and (19). The Newton method has a sufficiently good rate of convergence; however, when using this approach, problems with the radius of convergence may occur. Thus, it is necessary to use a priori information about the structure of the solitary waves we are looking for. Because the lattice equations (6) with nearest-neighbor Laplacian coupling can be considered as a specific approximation for the corresponding continuous model (16) with the kernel (15),

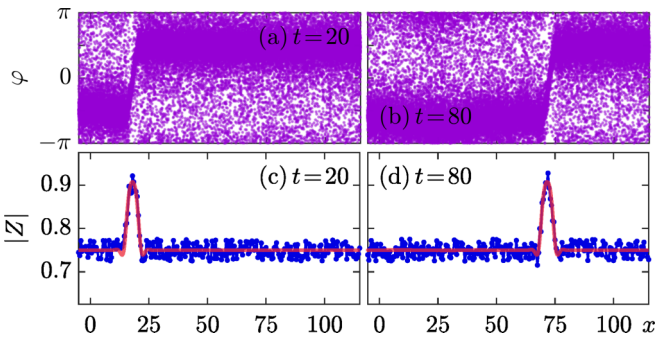

FIG. 6. Solitary wave simulated in the model (14) with $G(x) = 2(x^2-1)e^{-x^2/2}$ and $\alpha = -\pi/2$. (a, b) Instantaneous phases. (c, d) Amplitude of the coarse-grained order parameter, locally averaged with a Gaussian kernel $e^{-x^2/2\varsigma^2}$ with $\varsigma = 0.025$ (blue line with dots). The red bold line shows the evolution of the corresponding soliton with $\lambda = 0.91$ on top of $\varrho = 0.75$ within Eq. (16). One can see the kink of the order parameter phase and the increased synchrony level within this kink.

it is natural to obtained this relevant information from our previous analysis performed in the framework of Eqs. (6). To this end, we first of all set $\mathcal{A} = 2\sigma^2$ and $\sigma = 1/\sqrt{3}$. In this case, the function $G(x)$ reaches its maximum (which is approximately equal to 0.8925) in points $x = \pm 1$, and the minimum value of $G(x)$ is -2. We take one of the localized solutions of (6) as a starting approximation for the Newton iterative procedure. As a result, we numerically obtain a representative of the class of traveling localized solutions of the integro-differential equation (16) with the kernel $G(x)$ in the form (15) with $\mathcal{A} = 2\sigma^2$ and $\sigma = 1/\sqrt{3}$. After that, in order to construct solitary synchronization waves for another values of σ, we implement the control-parameter continuation ideology in the numerical calculations, which allows us to remain in the convergence domain for the Newton method.

We illustrate in Fig. 6 the found solitary wave, together with direct numerical simulations of the phase model (14) (where for computational purposes we utilized discretization of continuous variable x with grid size $\ell = 0.00025$ and used randomzsed phases similar to Fig. 5). One can see that the solitary synchronization wave is robust despite the finite-size fluctuations due to a finite mesh.

IV. CONCLUSION

In conclusion, we have described solitary synchronization waves in an array of oscillators with Laplacian coupling. These waves are propagating with a constant velocity profiles of the complex order parameter; they can be characterized as kinks of the global phase, and within these kinks the local synchronization level is higher than in the surrounding background. In the limit of a fully synchronized background, only the phase kinks remain, which coincide with previously studied compactons and kovatons.

We presented traveling localized solutions for the simplest lattice model, and demonstrated that they are also robust in large populations with integral coupling terms. For identical oscillators with conservative coupling, there is a family of solitons with different velocities on different backgrounds, similar to other conservative nonlinear wave systems such as the NLS lattice. For nonidentical elements, a finite level of synchrony can be maintained by attractive coupling; here the solitary synchronization waves are dissipative solitons. A more detailed analysis of this case will be presented elsewhere.

While we focused only on solitary waves in this paper, we can mention that general initial conditions typically lead to rather complex, turbulent patterns of the order parameter. If the initial profile is a localized bump on a constant background, typically at the propagating edges a system of solitary waves is formed, and at large times the leading soliton with the largest velocity is well separated from the waves behind it. We, however, have not studied interactions and collisions of the solitary waves.

ACKNOWLEDGMENTS

We thank P. Rosenau and A. Nepomnyashchy for fruitful discussions. L.A.S. thanks the DAAD for support (Grant No. 91697213). The analytical and numerical study of solitary synchronization waves in a lattice of nearest-neighbor interacting subensembles of globally coupled elements (Sec. II) was supported by the Russian Science Foundation (Grant No. 17-12-01534). The numerical evidence of such traveling localized waves in a one-dimensional medium of nonlocally coupled phase oscillators (Sec. III) was supported by the Russian Science Foundation (Grant No. 14-12-00811).

[1] Y. Kuramoto, in *International Symposium on Mathematical Problems in Theoretical Physics*, edited by H. Araki, Lecture Notes in Physics Vol. 39 (Springer, New York, 1975), p. 420; J. A. Acebrón, L. L. Bonilla, C. J. P. Vicente, F. Ritort, and R. Spigler, Rev. Mod. Phys. **77**, 137 (2005).

[2] M. Nixon, E. Ronen, A. A. Friesem, and N. Davidson, Phys. Rev. Lett. **110**, 184102 (2013); I. Kiss, Y. Zhai, and J. Hudson, Science **296**, 1676 (2002); A. A. Temirbayev, Z. Z. Zhanabaev, S. B. Tarasov, V. I. Ponomarenko, and M. Rosenblum, Phys. Rev. E **85**, 015204(R) (2012); A. Prindle, P. Samayoa, I. Razinkov, T. Danino, L. S. Tsimring, and J. Hasty, Nature (London) **481**, 39 (2012).

[3] M. J. Panaggio and D. M. Abrams, Nonlinearity **28**, R67 (2015); O. E. Omel'chenko, *ibid.* **31**, R121 (2018).

[4] Y. Kuramoto and D. Battogtokh, Nonlinear Phenom. Complex Syst. **5**, 380 (2002).

[5] M. R. Tinsley, S. Nkomo, and K. Showalter, Nat. Phys. **8**, 662 (2012); E. A. Martens, S. Thutupalli, A. Fourrière, and O. Hallatschek, Proc. Natl. Acad. Sci. U. S. A. **110**, 10563 (2013).

[6] S. Nkomo, M. R. Tinsley, and K. Showalter, Phys. Rev. Lett. **110**, 244102 (2013); J. F. Totz, J. Rode, M. R. Tinsley, K. Showalter, and H. Engel, Nat. Phys. **14**, 282 (2018).

[7] D. M. Abrams, R. Mirollo, S. H. Strogatz, and D. A. Wiley, Phys. Rev. Lett. **101**, 084103 (2008); A. Pikovsky and

M. Rosenblum, *ibid.* **101**, 264103 (2008); E. A. Martens, M. J. Panaggio, and D. M. Abrams, New J. Phys. **18**, 022002 (2016); E. A. Martens, C. Bick, and M. J. Panaggio, Chaos **26**, 094819 (2016); T. Kotwal, X. Jiang, and D. M. Abrams, Phys. Rev. Lett. **119**, 264101 (2017).

[8] E. A. Martens, Phys. Rev. E **82**, 016216 (2010); Chaos **20**, 043122 (2010).

[9] E. Ott and T. M. Antonsen, Chaos **18**, 037113 (2008).

[10] G. Bordyugov, A. Pikovsky, and M. Rosenblum, Phys. Rev. E **82**, 035205 (2010); C. R. Laing, Physica D **240**, 1960 (2011); L. Smirnov, G. Osipov, and A. Pikovsky, J. Phys. A **50**, 08LT01 (2017).

[11] J. C. Eilbeck and M. Johansson, in *Proc. 3rd Conf. Localization and Energy Transfer in Nonlinear Systems*, edited by L. Vazquez, R. S. MacKay, and M. P. Zorzano (World Scientific, Singapore, 2003), pp. 44–67.

[12] P. Rosenau and A. Pikovsky, Phys. Rev. Lett. **94**, 174102 (2005); A. Pikovsky and P. Rosenau, Physica D **218**, 56 (2006); K. Ahnert and A. Pikovsky, Chaos **18**, 037118 (2008).

[13] Y. Kuramoto and S.-I. Shima, Prog. Theor. Phys. Suppl. **150**, 115 (2003); S.-I. Shima and Y. Kuramoto, Phys. Rev. E **69**, 036213 (2004); C. R. Laing, *ibid.* **92**, 050904 (2015); C. Laing, SIAM J. Appl. Dyn. Syst, **16**, 974 (2017); B.-W. Li and H. Dierckx, Phys. Rev. E **93**, 020202 (2016).